

Multiple Folding Pathways of the SH3 domain

Jose M. Borreguero¹, Feng Ding¹, Sergey V. Buldyrev¹, H. Eugene Stanley¹,
and Nikolay V. Dokholyan²

March 31, 2002

¹Center for Polymer Studies and Department of Physics,
Boston University, Boston, MA 02215 USA

²Department of Biochemistry and Biophysics, School of Medicine,
University of North Carolina at Chapel Hill, Chapel Hill, NC 27599

Abstract

Experimental observations suggest that proteins follow different pathways under different environmental conditions. We perform molecular dynamics simulations of a model of the SH3 domain over a broad range of temperatures, and identify distinct pathways in the folding transition. We determine the kinetic partition temperature — the temperature for which the SH3 domain undergoes a rapid folding transition with minimal kinetic barriers — and observe that below this temperature the model protein may undergo a folding transition via multiple folding pathways. The folding kinetics is characterized by slow and fast pathways and the presence of only one or two intermediates. Our findings suggest the hypothesis that the SH3 domain, a protein for which only two-state folding kinetics was observed in previous experiments, may exhibit intermediate states under extreme experimental conditions, such as very low temperatures. A very recent report (Viguera et al., Proc. Natl. Acad. Sci. USA, 100:5730–5735, 2003) of an intermediate in the folding transition of the Bergerac mutant of the α -spectrin SH3 domain protein supports this hypothesis.

Keywords: intermediate, molecular dynamics, folding pathways, SH3, kinetic partition.

Corresponding author. E-mail: jnborr@bu.edu

INTRODUCTION

Recent experimental studies indicate that several proteins exhibit simultaneously a variety of intermediates and folding pathways. Kiefhaber¹ identified at low denaturant concentration a fast pathway (50 ms) in the folding of lysozyme with no intermediates and a slow phase (420 ms) with well-populated intermediates. Choe et al.² observed the formation of a kinetic intermediate in the folding of villin 14T upon decreasing the temperature, and Silverman et al.³ observed the extinction of a slow phase in the folding of the P4-P6 domain upon changes in ion concentration. Kitahara et al.⁴ studied a pressure-stabilized intermediate of ubiquitin, identified as an α -pathway intermediate in previous kinetics experiments at basic conditions⁵. All these studies suggest that environmental conditions favor some folding pathways over others.

Major theoretical efforts in the study of protein folding⁶⁽¹⁶⁾ have focused on small, single domain proteins¹⁷. It is found in experiments^{17,18} that these proteins undergo folding transition with no accumulation of kinetic intermediates in the accessible range of experimental conditions. However, other kinetics studies of two-state proteins¹⁹⁽²²⁾ suggest the presence of short-lived intermediates that cannot be directly detected experimentally. Recently, Sanchez et al.²³ explained the curved Chevron plots | the non-linear dependence of folding and unfolding rates on denaturant concentration²⁴⁽²⁶⁾ | of 17 selected proteins by assuming the presence of an intermediate state. Led by these studies, we hypothesize that single domain proteins may exhibit intermediates in the folding transition under suitable environmental conditions.

To test our hypothesis, we perform a molecular dynamics study of the folding pathways of the c-Crk SH3 domain²⁷⁽²⁹⁾ (PDB²⁹ access code 1cka). The SH3 domain is a family of small globular proteins which has been extensively studied in kinetics and thermodynamic experiments^{18,30(37)}. We select the c-Crk SH3 domain (57 residues) as the SH3 domain representative and perform molecular dynamics simulations over a broad range of temperatures. We determine the kinetic partition temperature^{12,38} T_{KP} below which the model protein exhibits slow folding pathways and above which the protein undergoes a cooperative folding transition with no accumulation of intermediates. Below T_{KP} , we study the presence of intermediates in the slow folding pathways and resolve their structure. We find that one of the intermediates populates the folding transition for temperatures as high as T_{KP} . We discuss the relevance of

our results in light of recent experimental evidence.

RESULTS

The SH3 domain is a β -sheet protein (upper triangle of Fig. 1a). Our previous thermodynamic studies⁶ of the c-Crk SH3 domain revealed only two stable states at equilibrium conditions: folded and unfolded. Both states coexist with equal probability at the folding transition temperature, $T_F = 0.526$, at which the temperature dependence of the potential energy has a sharp change, and the specific heat has a maximum (experimentally¹⁸, this temperature corresponds to 67 C). Thus, our model reproduces the experimentally-determined thermodynamics of the SH3 domain^{18,30,31}.

Initial Unfolded Ensemble

Our initially unfolded ensemble consists of 1100 protein conformations that we sample from a long equilibrium simulation at a high temperature $T_0 = 1.0$ at equal time intervals of 10^4 time units (t.u.). This time separation is long enough to ensure that the sampled conformations have low structural similarity among themselves. We calculate the frequency map | the plot of the probability of any two amino acids forming a contact | of this unfolded ensemble (lower triangle of Fig. 1a). At $T = 1.0$, only nearest and next nearest contacts have high frequency, and the frequency decreases rapidly with the sequence separation between the amino acids.

When we quench the system from $T = 1.0$ to a target temperature, T_{target} (see Methods), the system relaxes in approximately 1500 t.u. Due to the finite size of our heat bath, the heat released by the protein upon folding increases the final temperature of the system by 0.03 units above T_{target} . After relaxation, the protein stays for a certain time in the unfolded state, then undergoes a folding transition. During this time interval, the protein explores unfolded conformations, and we calculate the frequency map of the unfolded state for different target temperatures.

At $T_{target} = T_F$, the secondary structure is unstable (Fig. 1b), with average frequency $f = 0.24$ (see Methods). Successful folding requires the cooperative formation of contacts throughout the protein in a nucleation process^{6,7}. At $T_{target} = 0.54$, the secondary structure is more stable (Fig. 1c, $f = 0.50$). Thus, the conformational search for the native state (NS) is optimized by limiting the search to the formation of a sufficient number of long range contacts. At $T_{target} = 0.33$, the lowest temperature studied, secondary structure elements form during the rapid collapse of the model protein in the first 1500 t.u.

(Fig. 1d, $f = 0.73$). During collapse, some tertiary contacts | contacts between secondary elements | may also form. The formation of these contacts prior to the proper arrangement of secondary structure elements may lead the protein model to a kinetic trap. Finally, folding proceeds at this temperature through a thermally activated search for the NS.

Kinetic Partition Temperature

In order to determine the temperature below which we can distinguish fast and slow folding pathways, we compute the distribution of folding times $p(t_F; T)$ (Fig. 2a(e), as well as the average $\langle t_F \rangle$ (Fig. 2f) and standard deviation σ_F . The ratio $r(T) = \langle t_F \rangle / \sigma_F$ measures the average folding time in units of the standard deviation σ_F . This quantity is particularly useful when the value of the standard deviation correlates with the value of the average as we change T_{target} . For instance, single-exponential distributions $e^{-t_F / \langle t_F \rangle} = e^{-t_F / \sigma_F}$ have $r = 1$.

We expect $r \ll 1$ for $T_{\text{target}} > T_F$, because at these high temperatures the folding transitions become rare events and are single-exponential distributed. As we decrease T_{target} , we expect $r > 1$ just below T_F , because the folded state becomes more stable than the unfolded state, and the folding transitions are favored. Distributions with $r > 1$ indicate a narrow distribution centered in $\langle t_F \rangle$, so that most of the simulations undergo a folding transition for times of the order of the average folding time. However, if we continue decreasing T_{target} , we expect some folding transitions to be kinetically trapped, and the folding time distribution will spread over several orders of magnitude. Such distributions have $r < 1$. Thus, there is a temperature below T_F where the maximum of $r(T)$ occurs, and which signals the onset of slow folding pathways. We use the maximum of $r(T)$ to calculate T_{KP} .

Fig. 2g suggests that $T_{KP} = 0.54$, which corresponds to a maximally compact distribution of folding times (Fig. 2d). We find that the ratio approaches one as we increase the temperature above T_{KP} , and the distribution of folding times approximates a single-exponential distribution. In particular, the distribution of folding times fits the single-exponential distribution $e^{-t_F / \langle t_F \rangle} = e^{-t_F / \sigma_F}$ for $T = 0.64$, the closest temperature to T_F that we study. The ratio $r(T)$ decreases monotonically below T_{KP} , indicating that the distribution of folding times spreads over several orders of magnitude. This is the consequence of an increasing fraction of folding simulations

kinetically trapped (Fig. 2a-b). The average folding time $\langle t_F \rangle$ is minimum not at T_{KP} , but at a lower temperature $T_{\langle t_F \rangle} = 0.49$ (Fig. 2f). At this temperature, we find that the protein becomes temporarily trapped in approximately 7% of the folding transitions. On the other hand, the remaining simulations undergo a folding transition much faster, thus minimizing $\langle t_F \rangle$. Interestingly, $r(T_{\langle t_F \rangle}) \approx 1.0$, even though the distribution of folding times at this temperature is non-exponential.

Folding Pathways

Below T_{KP} , an increasing fraction of the simulations undergo folding transitions that take a time up to three orders of magnitude above the minimum $\langle t_F \rangle$. In addition, $\langle t_F \rangle$ increases dramatically (Fig. 2f). At the lowest temperatures studied, we distinguish between the majority of simulations that undergo a fast folding transition (the fast pathway) and the rest of the simulations that undergo folding transitions with folding times spanning three orders of magnitude (the slow pathways). At the low temperature $T = 0.33$, the potential energy of the fast pathway has on average the same time evolution of all the simulations at $T_{KP} = 0.54$, indicating that there are no kinetic traps in the fast pathway.

For each folding simulation that belongs to the slow pathways, we sample the potential energy at equal time intervals of 100 t.u. until folding is finished (see Methods). Then, we collect all potential energy values and construct a distribution of potential energies. We find that below $T = 0.43$, the distribution is markedly bimodal (Fig. 3a). The positions of the two peaks along the energy coordinate do not correspond to the equilibrium potential energy value of the folded state (Fig. 3b). Therefore we hypothesize the existence of two intermediates in the slow pathways. We denote the two putative intermediates as I_1 and I_2 for the high energy and low energy peaks, respectively. As temperature decreases, the peaks shift to lower energies, but the energy difference between the two peaks, approximately six energy units, remains constant (Fig. 3b). A constant energy difference implies that the two putative intermediates differ by a specific set of native contacts. As temperature decreases, other contacts not belonging to this set become more stable and are responsible for the overall energy decrease. At $T = 0.33$, we record the distribution of survival times for both intermediates and find that they fit a single-exponential distribution, supporting the hypothesis that each intermediate is a local free energy minimum and has a major free energy barrier (Fig. 3c).

¹⁸ Assuming a linear relation between experimental and simulated temperatures and taking into account¹⁸ that $T_F = 67$ C, we estimate $T_{KP} \approx 20$ C

To further test the single free energy barrier hypothesis, we select a typical conformation representing intermediate I_2 and perform 200 folding simulations, each with a different set of initial velocities for a set of temperatures in the range $0.33 \leq T \leq 0.52$. For each simulation, we record the time that the protein stays in the intermediate and find that the average survival time fits the Arrhenius law for temperatures below $T = 0.44$ (Fig. 3d). This upper bound temperature roughly coincides with the temperature $T = 0.43$ below which I_2 becomes noticeable in the histogram of potential energies (Fig. 3a). This result indicates that the free energy barrier to overcome intermediate I_2 becomes independent of temperature for low temperatures, or analogously, that the same set of native contacts must form (or break) to overcome the intermediate.

Next, we determine the structure of the two intermediates. For each intermediate, we randomly select three conformations and find that they are structurally similar. Conformations belonging to intermediate I_1 have a set of long-range contacts (C_1) with a high occupancy and a set of long-range contacts (C_2) with no occupancy at all (Fig. 3e). Contacts in C_1 represent a β -sheet made by three strands: the two termini and the strand following the RT-loop, which we name strand "A" (see I_1 in Fig. 4). Contacts in C_2 represent the base of the n-Src loop and the contacts between the RT-loop and the distal hairpin (see I_2 in Fig. 4). In addition, I_1 has a set of medium-range contacts (C_3) with high occupancy (Fig. 3e) representing the distal hairpin and a part of the n-Src loop. For a slow folding transition, the β -sheet (C_1 contacts) forms in the early events and strand "A" can no longer move freely. This constrained motion prevents strand "A" from forming contacts with one of the strands of the distal hairpin, which we name as strand "B" (see I_2 in Fig. 4). Similarly, strand "B" cannot move freely because it is a part of C_3 . The missing contacts between strand "A" and strand "B" are the contacts that form the base of the n-Src loop.

Conformational changes leading the protein away from intermediate I_1 involve either dissociation of the β -sheet, thus breaking some contacts of C_1 , or dissociation of the distal hairpin, thus breaking some contacts of C_3 . We find that the latter dissociation may lead the protein conformation to intermediate I_2 . Intermediate I_2 has contacts of C_1 , but lacks the set of contacts (C_4) that form the base of the distal hairpin (see NS in Fig. 4).

Once we identify the structure of the intermediates, we investigate whether intermediate I_1 is present at larger temperatures when no distinction can be made concerning fast and slow folding pathways. To

test this hypothesis, we sample the protein conformation during the folding transition at equal time intervals of 60 t.u. for each of the 1100 simulations, and compare these conformations to intermediate I_1 with a similarity score function (see Methods). For each folding transition, we record only the highest value of the similarity score, thus obtaining 1100 highest score values. At T_{KP} , the histogram of the highest scores is bimodal, with 25% of the folding simulations passing through intermediate I_1 (Fig. 3f). We find that at T_{KP} , simulations that undergo the folding transition through I_1 show kinetics of folding no different than those of the rest of simulations.

DISCUSSION

It was shown⁶ that the simplified protein model and interaction potentials that we use here reproduced in a certain range of temperatures the experimentally-determined two-state thermodynamics of the SH3 domain¹⁸. The qualitative predictive power of the model encouraged us to study the folding kinetics in a wider range of temperatures. From our relaxation studies of the initial unfolded ensemble, we observe that the structure of the unfolded state is highly sensitive to T_{target} . The role of the unfolded state in determining the folding kinetics has already been pointed out in recent experimental and theoretical studies^{39,42}. We observe nucleation⁶, folding with minimal kinetic barriers, and thermally activated mechanisms for the different observed unfolded states.

In previous studies, various methods have been developed to determine the temperature that signals the onset of slow folding pathways. Socci et al.^{43,44} determined a glass transition temperature, T_g , at which the average folding time is halfway between t_{min} and t_{max} , where t_{min} is the minimum average folding time and t_{max} is the total simulation time. This method is sensitive to the a priori selected t_{max} . The authors varied t_{max} in the range $0.27 \cdot 10^9 < t_{max} < 0.960 \cdot 10^9$, and they found a 10% error in the calculation of T_g . Also, Gutin et al.⁴⁵ estimated a critical temperature, T_c , at which the temperature dependence of the equilibrium potential energy leveled off. From their results, one can evaluate a 20% error in their calculation of T_c . Both T_g and T_c are temperatures that authors use to characterize the onset of multiple folding pathways. In our study we use T_{KP} , which signals the breaking of time translational invariance of equilibrium measurements for temperatures below this value⁴⁶. We estimate a 2% error in our calculation of T_{KP} from uncertainties in the location of T_{KP} in Fig. 2g.

At T_{KP} , secondary structure elements are partially stable, and the search for the NS reduces to the formation of tertiary contacts. Furthermore, T_{KP} is a relatively high temperature that prevents the stabilization of improper arrangements of the protein conformation, thus minimizing the occurrence of kinetic traps. Below T_{KP} , the model protein exhibits two intermediates with well-defined structural characteristics. This modest number of intermediates is a direct consequence of the prevention of non-native contacts. This prevention reduces dramatically the number of protein conformations. Furthermore, since a low energy value implies that most of the native interactions have formed, there are few conformations having both low energy and structural differences with the NS¹.

It is found experimentally^{13,47,54} that proteins exhibit only a discrete set of intermediates. Even though in real proteins amino acids that do not form a native contact may still attract each other, experimental and theoretical studies confirm that native contacts have a leading role in the folding transition. Protein engineering experiments^{33,55,58} show that transition states in two-state globular proteins are mostly stabilized by native interactions. To quantitatively determine the importance of native interactions in the folding transition, Paci et al.⁵⁹ studied the transition states of three two-state proteins with a full-atom model. They found that on average, native interactions accounted for approximately 83% of the total energy of the transition states. Of relevance to our studies of the SH3 domain are the full-atom study⁶⁰ and the protein engineering experiments^{33,36} showing that the transition state of the src-SH3 domain protein is determined by the NS. On the other hand, evidence exists that in some proteins, non-native contacts are responsible for the presence of intermediates. In their study of the homologous Im7 and Im9 proteins, Capaldi et al.⁶¹ identified a set of non-native interactions responsible for an intermediate state in the folding transition of Im7 protein. Miyayama et al.⁶² performed Monte Carlo simulations of two different sequences with the same NS in the 3×3 lattice. One sequence presented a series of pathways with misfolded states due to non-native interactions.

We investigate the kinetics of formation of the two intermediates in a wide range of temperatures. At low temperatures, simulations that undergo folding through intermediate I_1 reveal that contacts between the two termini form earlier than the contacts belonging to the folding nucleus^{6,7}. This result coincides with an α -lattice study⁶³ of a 36-monomer protein by Abkevich et al. In this study, the authors found an intermediate in the folding transition of their model protein. Inspection of the interme-

diates revealed no nucleus contacts, but a different set of long-range contacts already formed. In addition, we learned of the work by Viguera et al.⁶⁴ after completion of our study. They reported that a mutant of the α -spectrin SH3 domain undergoes a folding transition through one intermediate. The authors observed that the newly-introduced long-range contacts had already been formed in the denatured state, preceding the formation of the transition state of the protein. Thus, environmental conditions that favor stabilization of long-range contacts other than the nucleus contacts may induce intermediates in the folding transition.

Alternatively, short-range contacts in key positions of the protein structure may also be responsible for slow folding pathways. After completion of our study, Karanicolas et al.^{65,66} reported their studies on the G α model of the forming binding protein WW domain. The authors found a slow folding pathway in the model protein, and a cluster of four short-range native contacts that are responsible for this pathway. However, the authors observed that it was the absence, not the presence, of these native contacts in the unfolded state that generated bi-phasic folding kinetics. Thus, environmental conditions that favor destabilization of short range contacts may promote the formation of intermediate states in the folding transition.

We also investigate the survival time of intermediate I_2 , and find that the free energy barrier separating I_2 from the NS is independent of temperature. Thus, the average survival time follows Arrhenius kinetics. The value of the free energy barrier is approximately 5.85 energy units, indicating that about six native contacts break when the protein conformation reaches the transition state that separates I_2 from the NS. At the low temperatures where intermediates I_1 and I_2 are noticeable, thermal fluctuations are still large enough so that the observed survival times of I_2 should be much smaller, if only any six native contacts were to break. Thus we hypothesize that it is always the same set of native contact that must break in the transition $I_2 \rightarrow NS$. Our observations of the transition $I_1 \rightarrow I_2$ support this hypothesis. In this transition, we find that the set of contacts C_4 always breaks.

At T_{KP} , we do not detect the intermediates from kinetics measurements of the average folding time, or analogously, from the folding rate. Thus we analyze the folding transition with the similarity score function that tests the presence of intermediate I_1 . Then we find that this intermediate is populated in 25% of the folding transitions. In a recent study⁶⁷, Gorski et al. reported the existence of an interme-

mediate in the folding transition of protein Im 9 under acidic conditions (pH = 5.5). This finding led authors to formulate the hypothesis that Im 9 has an intermediate at normal conditions (pH = 7.0), but it is too unstable to be detected with current kinetic experimental techniques. Interestingly, the homologous protein Im 7 (60% sequence identity) undergoes folding transition through an intermediate in all tested experimental conditions^{61,67,68}, supporting the authors' hypothesis. Thus, changes in both the environmental conditions and the amino acid sequence may uncover hidden intermediates in the folding transition of a two-state protein. In addition, a detailed study at T_{K_P} may reveal the intermediates. This is particularly useful for computer simulations, because simulations at low temperatures when intermediates are easily identifiable may require several orders of magnitude longer than simulations at T_{K_P} .

Conclusion

We perform molecular dynamics analysis of the folding transition of the G_o model of the c-Crk SH3 domain in a broad range of temperatures. At the folding transition temperature, we observe that only the folded and unfolded states are populated. However, as we decrease the temperature, parameters monitoring the folding process such as potential energy and root mean square distance with respect to the native state, r_{msd} , suggest the presence of intermediates. We determine the kinetic partition temperature T_{K_P} below which we observe two folding intermediates, I_1 and I_2 , and above which we do not observe accumulation of intermediates. Below T_{K_P} , intermediate I_1 forms when the two termini and the strand following the RT-loop form a β -sheet, prior to the formation of the folding nucleus. This intermediate effectively splits the folding transition into fast and slow folding pathways. Dissociation of part of the β -sheet leads the protein to the native state. We also find that stabilization of this β -sheet and subsequent dissociation of the distal hairpin may lead to intermediate I_2 .

The key structural characteristics of intermediate I_1 allow us to define a similarity score function that probes the presence of the intermediate in a folding transition. We find that I_1 is populated even at T_{K_P} . This result suggests that one can obtain information regarding the existence of putative intermediates by studying the folding trajectories at T_{K_P} . However, at this temperature, no intermediates are noticeable if one limits the analysis only to the distribution of folding times.

We observe that the folding pathways of the model SH3 domain are highly sensitive to temperature, suggesting the important role of the environmental con-

ditions in determining the folding mechanism. Our findings suggest that the SH3 domain, a two-state folder, may exhibit stable intermediates under extreme experimental conditions, such as very low temperatures.

MATERIALS AND METHODS

Model Protein and Interactions

We adopt a coarse-grained description of the protein by which each amino acid is reduced to its C_α atom (C_β in case of Gly). Details of the model, the surrounding heat bath, and the selection of structural parameters are discussed in detail in a previous study⁶. The selection of the set of interaction parameters among amino acids is of crucial importance for the resulting folding kinetics of the model protein^{11,12,14}. Experimental and theoretical studies of globular proteins^{6,7,36,57,69,76} suggest that native topology is the principal determinant of the folding mechanism. Thus, we employ a variant of the G_o model of interactions^{12,77,81} — a model based solely on the native topology — in which we prevent formation of non-native interactions, since we are solely interested in the role that native topology and native interactions may have in the formation of intermediates. We perform simulations and monitor the time evolution of the protein and the heat bath with the discrete molecular dynamics algorithm^{82,88}. The higher performance of this algorithm over conventional molecular dynamics allows one to increase the computational speed up to three orders of magnitude.

Frequencies and Folding Simulations

To calculate the frequency map at $T = 1.0$, we probe the presence of the native contacts in each of the 1100 initially unfolded conformations. Then, we compute the probability of each native contact to be present. To calculate the frequency map at T_{target} , we select one particular folding transition and we probe the presence of the native contacts during the time interval that spans after the initial relaxation and before the simulation reaches the folding time t_F . To compute t_F , we stop the folding simulation when 90% of the native contacts form. Then, we trace back the folding trajectory and record t_F when the root mean square distance with respect to the native state, r_{msd} , becomes smaller than 3Å . We consider all protein conformations occurring for $t > t_F$ as belonging to the folded state and of no relevance to the folding

transition.

Similarity Score Function

We introduce the similarity score function, $S = \frac{a}{a+b}$, where a is the number of native contacts belonging to the set of contacts C_1 , and b is the number of native contacts belonging to set C_2 (Fig. 3e). C_1 has 23 contacts and C_2 has 15 contacts. If the protein is unfolded, then $a = b = 0$, thus $S = 0$. Similarly, if the protein is folded, then $a = 23$ and $b = 15$, thus $S = 0.6$ again. Finally, if the protein adopts the intermediate I_1 structure, then $a = 23$ and $b = 0$, thus $S = 1$.

We acknowledge E. I. Shakhnovich for insightful discussions, R. Badzey for careful reading of the manuscript, and the Petroleum Research Fund for support.

References

1. Kiefhaber, T. (1995). Kinetics traps in Lysozyme folding. *Proc. Natl. Acad. Sci. USA*, 92, 9029{9033.
2. Choe, S.E., Matsudaira, P.T., Osterhout, J., Wagner, G. & Shakhnovich, E.I. (1998). Folding kinetics of villin 14T, a protein domain with a central beta-sheet and two hydrophobic cores. *Biochemistry*, 37, 14508{14518.
3. Silverman, S.K., Deras, M.L., Woodson, S.A., Scaringe, S.A. & Cech, T.R. (2000). Multiple folding pathways for the p4-p6 RNA domain. *Biochemistry*, 39, 12465{12475.
4. Kitahara, R. & Akasaka, K. (2003). Close identity of a pressure-stabilized intermediate with a kinetic intermediate in protein folding. *Proc. Natl. Acad. Sci. USA*, 100, 3167{3172.
5. Riggs, M.S. & Roder, H. (1992). Early hydrogen-bonding events in the folding reaction of ubiquitin. *Proc. Natl. Acad. Sci. USA*, 89, 2017{2021.
6. Borreguero, J.M., Dokholyan, N.V., Buldyrev, S.V., Shakhnovich, E.I. & Stanley, H.E. (2002). Thermodynamics and folding kinetics analysis of the SH3 domain from discrete molecular dynamics. *J. Mol. Biol.* 318, 863{876.
7. Ding, F., Dokholyan, N.V., Buldyrev, S.V., Stanley, H.E. & Shakhnovich, E.I. (2002). Direct molecular dynamics observation of protein folding transition state ensemble. *Biophys. J.* 83, 3525{3532.
8. Fersht, A.R. & Daggett, V. (2002). Protein folding and unfolding at atomic resolution. *Cell*, 108, 573{582.
9. Karplus, M. & McCammon, J.A. (2002). Molecular dynamics simulations of biomolecules. *Nature Struct. Biol.* 9, 646{652.
10. Ozkan, S.B., Dill, K.A. & Bahar, I. (2002). Fast folding protein kinetics, hidden intermediates, and the sequential stabilization model. *Prot. Sci.* 11, 1958{1970.
11. Plotkin, S.S. & Onuchic, J.N. (2002). Structural and energetic heterogeneity in protein folding. I. theory. *J. Chem. Phys.* 116, 5263{5283.
12. Thirumalai, D., Klimov, D.K. & Dima, R.I. (2002). Insights into specific problems in protein folding using simple concepts. *Adv. Chem. Phys.* 120, 35{76.
13. Tiana, G. & Broglia, R.A. (2001). Statistical analysis of native contact formation in the folding of designed model proteins. *J. Chem. Phys.* 114, 2503{2510.
14. Pande, V.S., Grosberg, A.Y. & Tanaka, T. (2000). Heteropolymer freezing and design: towards physical models of protein folding. *Rev. Mod. Phys.* 72, 259{314.
15. Eaton, W.A., Muñoz, V., Hagen, J.S.J., Jas, G.S., Lapidus, L.J., Henry, E.R. & Hofrichter, J. (2000). Fast kinetics and mechanisms in protein folding. *Annu. Rev. Biophys. Biomol. Struct.* 29, 327.
16. Bryngelson, J.D. & Wolynes, P.G. (1989). Intermediates and barrier crossing in a random energy model (with applications to protein folding). *J. Phys. Chem.* 93, 6902{6915.
17. Jackson, S.E. (1998). How do small single-domain proteins fold? *Folding & Design*, 3, R81{R91.
18. Filimonov, V.V., Azuaga, A.I., Viguera, A.R., Serrano, L. & Mateo, P.L. (1999). A thermodynamic analysis of a family of small globular proteins: SH3 domains. *Biophys. Chem.* 77, 195{208.
19. Chiti, F., Taddei, N., White, P.M., Bucciantini, M., Magerini, F., Stefani, M. & Dobson, C.M. (1999). Mutational analysis of acylphosphatase suggests the importance of topology and contact order in protein folding. *Nature Struct. Biol.* 6, 1005{1009.
20. Houlston, R.S., Liu, C.S., Singh, L.M.R. & Meiering, E.M. (2002). pH and urea dependence of amide hydrogen-deuterium exchange rates in the beta-trefoil protein histactophilin. *Biochemistry*, 41, 1182{1194.
21. Khorasanizadeh, S., Petrus, I.D. & Roder, H. (1996). Evidence for a three-state model of protein folding from kinetics analysis of ubiquitin variants with altered core residues. *Nature Struct. Biol.* 3, 193{205.
22. Bachmann, A. & Kiefhaber, T. (2001). Apparent two-state tandem folding is a sequential process along a defined route. *J. Mol. Biol.* 306, 375{386.

23. Sanchez, I.E. & Kiefhaber, T. (2003). Evidence for sequential barriers and obligatory intermediates in apparent two-state protein folding. *J. Mol. Biol.* 325, 367{376.
24. Ikai, A. & Tandford, C. (1973). Kinetics of unfolding and refolding of proteins. *Mathematical analysis.* *J. Mol. Biol.* 73, 145{163.
25. Matouschek, A., Jr, J.T.K., Serrano, L., Bycroft, M. & Fersht, A.R. (1990). Transient folding intermediates characterized by protein engineering. *J. Mol. Biol.* 346, 440-445.
26. Fersht, A.R. (2000). A kinetically significant intermediate in the folding of barnase. *Proc. Natl. Acad. Sci. USA*, 97, 14121{14126.
27. Wu, X.D., Knudsen, B., Feller, S.M., Sali, J., Cowburn, D. & Hanafusa, H. (1995). Structural basis for the specific interaction of lysine-containing proline-rich peptides with the n-terminal SH3 domain of c-Crk. *Structure*, 2, 215{226.
28. Branden, C. & Tooze, J. (1999). *Introduction to Protein Structure.* Garland Publishing Inc, New York.
29. Bertram, H.M., Westbrook, J., Feng, Z., Gilliland, G., Bhat, T.N., Weissig, H., Shindyalov, I.N. & Bourne, P.E. (2000). The protein data bank. *Nucleic Acids Research*, 28, 235{242.
30. Viguera, A.R., Martinez, J.C., Filimonov, V.V., Mateo, P.L. & Serrano, L. (1994). Thermodynamic and kinetic analysis of the SH3 domain of Spectrin shows a 2-state folding transition. *Biochemistry*, 33, 10925{10933.
31. Villegas, V., Azuaga, A., Catusas, L., Reverter, D., Mateo, P.L., Aviles, F.X. & Serrano, L. (1995). Evidence for a 2-state transition in the folding process of the activation domain of human procarboxypeptidase-a2. *Biochemistry*, 46, 15105{15110.
32. Grantcharova, V.P. & Baker, D. (1997). Folding dynamics of the Src SH3 domain. *Biochemistry*, 36, 15685{15692.
33. Grantcharova, V.P., Riddle, D.S., Santiago, J.N. & Baker, D. (1998). Important role of hydrogen bonds in the structurally polarized transition state for folding of the src SH3 domain. *Nature Struct. Biol.* 8, 714{720.
34. Knapp, S., Mattson, P.T., Christova, P., Berndt, K.D., Karshiko, A., Vihinen, M., Smith, C.I. & Ladenstein, R. (1998). Thermal unfolding of small proteins with SH3 domain folding pattern. *Proteins: Struct. Func. & Genet.* 23, 309{319.
35. Martinez, J.C., Viguera, A.R., Berisio, R., Williams, M., Mateo, P.L., Filimonov, V.V. & Serrano, L. (1999). Thermodynamic analysis of alpha-spectrin SH3 and two of its circular permuted variants with different loop lengths: Discerning the reasons for rapid folding in proteins. *Biochemistry*, 38, 549{559.
36. Riddle, D.S., Grantcharova, V.P., Santiago, J.V., Ruczinski, A.E. & Baker, D. (1999). Experiment and theory highlight role of native state topology in SH3 folding. *Nature Struct. Biol.* 6, 1016{1024.
37. Guerois, R. & Serrano, L. (2000). The SH3-fold family: experimental evidence and prediction of variations in the folding pathways. *J. Mol. Biol.* 304, 967{982.
38. Klimov, D.K. & Thirumalai, D. (1996). Factors governing the foldability of proteins. *Proteins*, 26, 411{441.
39. Zagrovic, B., Snow, C.D., Khaliq, S., Shirts, M.R. & Pande, V.S. (2002). Native-like mean structure in the unfolded ensemble of small proteins. *J. Mol. Biol.* 323, 153{164.
40. Millet, I.S., Doniach, S. & Plaxco, K.W. (2002). Toward a taxonomy of the denatured state: Small angle scattering studies of unfolded proteins. *Adv. Protein Chem.* 62, 241{262.
41. Plaxco, K.W. & Gross, M. (2001). Unfolded, yes, but random? Never! *Nature Struct. Biol.* 8, 659{660.
42. Garcia, P., Serrano, L., Durand, D., Rico, M. & Bruix, M. (2001). NMR and SAXS characterization of the denatured state of the chemotactic protein CheY: Implications for protein folding initiation. *Prot. Sci.* 10, 1100{1112.
43. Soccia, N.D. & Onuchic, J.N. (1994). Folding kinetics of proteinlike heteropolymers. *J. Chem. Phys.* 101, 1519{1528.
44. Soccia, N.D., Onuchic, J.N. & Wolynes, P.G. (1996). Diffusive dynamics of the reaction coordinate for protein folding funnels. *J. Chem. Phys.* 15, 5860{5868.
45. Gutin, A., Sali, A., Abkevich, V., Karplus, M. & Shakhnovich, E.I. (1998). Temperature dependence of the folding rate in a simple protein model: search for a "glass" transition. *J. Chem. Phys.* 108, 6466{6483.

46. Dokholyan, N. V., Pitard, E., Buldyrev, S. V. & Stanley, H. E. (2002). Glassy behavior of a homopolymer from molecular dynamics simulations. *Phys. Rev. E*, 65, 030801{14}.
47. Bhutani, N. & Udgaonkar, J. B. (2001). GroEL channels the folding of thioredoxin along one kinetic route. *J. Mol. Biol.* 345, 1167{1179}.
48. Tezcan, F. A., Findley, W. M., Crane, B. R., Ross, S. A., Lyubovitsky, J. G., Gray, H. B. & Winkler, J. R. (2002). Using deeply trapped intermediates to map the cytochrome c folding landscape. *Proc. Natl. Acad. Sci. USA*, 99, 8626{8630}.
49. Juneja, J. & Udgaonkar, J. B. (2002). Characterization of the unfolding of ribonuclease A by a pulsed hydrogen exchange study: Evidence for competing pathways for unfolding. *Biochemistry*, 41, 2641{2654}.
50. Park, S. H., O'Neil, K. T. & Roder, H. (1997). An early intermediate in the folding reaction of the B1 domain of protein G contains a native-like core. *Biochemistry*, 36, 14277{14283}.
51. Segel, D. J., Bachmann, A., Hofrichter, J., Hodgson, K. O., Doniach, S. & Kiefhaber, T. (1999). Characterization of transient intermediates in lysozyme folding with time-resolved small-angle X-ray scattering. *J. Mol. Biol.* 288, 489{499}.
52. Heidary, D. K., O'Neill, J. C., Roy, M. & Jennings, P. A. (2000). An essential intermediate in the folding of dihydrofolate reductase. *Proc. Natl. Acad. Sci. USA*, 97, 5866{5870}.
53. Rumbley, J., Hoang, L., Mayne, L. & Englander, S. W. (2001). An amino acid code for protein folding. *Proc. Natl. Acad. Sci. USA*, 98, 105{112}.
54. Simmons, D. A. & Konermann, L. (2002). Characterization of transient protein folding intermediates during myoglobin reconstitution by time-resolved electrospray mass spectrometry with on-line isotopic pulse labeling. *Biochemistry*, 41, 1906{1914}.
55. Fersht, A. R. (1995). Characterizing transition-states in protein folding | an essential step in the puzzle. *Curr. Opin. Struct. Biol.* 1, 79{84}.
56. Temstrom, T., Mayor, U., Akke, M. & Oliveberg, M. (1999). From snapshot to movie: phi analysis of protein folding transition states taken one step further. *Proc. Natl. Acad. Sci. USA*, 96, 14854{14859}.
57. Clementi, C., Nymeyer, H. & Onuchic, J. N. (2000). Topological and energetic factors: what determines the structural details of the transition state ensemble and "en-route" intermediates for protein folding? An investigation for small globular proteins. *J. Mol. Biol.* 5, 937{953}.
58. Northey, J. G. B., Nardo, A. A. D. & Davidson, A. R. (2002). Hydrophobic core packing in the SH3 domain folding transition state. *Nature Struct. Biol.* 9, 126{130}.
59. Paci, E., Vendruscolo, M. & Karplus, M. (2002). Native and non-native interactions along protein folding and unfolding pathways. *Proteins: Struct. Func. & Genet.* 47, 379{392}.
60. Shea, J. E., Onuchic, J. N. & III, C. L. B. (2002). Probing the folding free energy landscape of the src-SH3 protein domain. *Proc. Natl. Acad. Sci. USA*, 99, 16064{16068}.
61. Capaldi, A. P., Kleinhous, C. & Radford, S. E. (2002). Im7 folding mechanism: misfolding on a path to the native state. *Nature Struct. Biol.* 9, 209{216}.
62. Minsky, L. A., Abkevich, V. & Shakhnovich, E. I. (1996). Universality and diversity of the protein folding scenarios: a comprehensive analysis with the aid of a lattice model. *Folding & Design*, 1, 103{116}.
63. Abkevich, V. I., Gutin, A. M. & Shakhnovich, E. I. (1994). Specific nucleus as the transition state for protein folding: evidence from the lattice model. *Biochemistry*, 33, 10026{10036}.
64. Viguera, A. R. & Serrano, L. (2003). Hydrogen-exchange stability analysis of Bergerac-Src homology 3 variants allows the characterization of a folding intermediate in equilibrium. *Proc. Natl. Acad. Sci. USA*, 100, 5730{5735}.
65. Karanicolas, J. & III, C. L. B. (2003). The structural basis for biphasic kinetics in the folding of the WW domain from a form-binding protein: Lessons for protein design? *Proc. Natl. Acad. Sci. USA*, 100, 3954{3959}.
66. Nguyen, H., Jager, M., Moretto, A., Guebele, M. & Kelly, J. W. (2003). Tuning the free-energy landscape of a WW domain by temperature, mutation, and truncation. *Proc. Natl. Acad. Sci. USA*, 100, 3948{3953}.

67. Gorski, S. A., Capaldi, A. P., Kleinhous, C. & Radford, S. E. (2001). Acidic conditions stabilise intermediates populated during the folding of Im 7 and Im 9. *J. Mol. Biol.* 312, 849{863.
68. Ferguson, N., Capaldi, A. P., James, R., Kleinhous, C. & Radford, S. E. (1999). Rapid folding with and without populated intermediates in the homologous four-helix proteins Im 7 and Im 9. *J. Mol. Biol.* 286, 1597{1608.
69. Pallaxo, K. W., Simons, K. T. & Baker, D. (1998). Contact order, transition state placement and the refolding rates of single domain proteins. *J. Mol. Biol.* 277, 985{994.
70. Munoz, V. & Eaton, W. A. (1999). A simple model for calculating the kinetics of protein folding from three-dimensional structures. *Proc. Natl. Acad. Sci. USA*, 96, 11311{11316.
71. Fersht, A. R. (2000). Transition-state structure as a unifying basis in protein-folding mechanism: contact order, chain topology, stability, and the extended nucleus mechanism. *Proc. Natl. Acad. Sci. USA*, 97, 1525{1529.
72. Alm, E. & Baker, D. (1999). Prediction of protein-folding mechanisms from free-energy landscapes derived from native structures. *Proc. Natl. Acad. Sci. USA*, 96, 11305{11310.
73. Galzitskaya, O. V. & Finkelstein, A. V. (1999). A theoretical search for folding/unfolding nuclei in three-dimensional protein structures. *Proc. Natl. Acad. Sci. USA*, 96, 11299{11304.
74. Shea, J. M., Onuchic, J. N. & Brooks, C. L. (2000). Energetic frustration and the nature of the transition state in protein folding. *J. Chem. Phys.* 113, 7663{7671.
75. Du, R., Pande, V. S., Grosberg, A. Y., Tanaka, T. & Shakhnovich, E. I. (1999). On the role of conformational geometry in protein folding. *J. Chem. Phys.* 111, 10375{10380.
76. Micheletti, C., Banavar, J. R., Maritan, A. & Seno, F. (1999). Protein structures and optimal folding from a geometrical variational principle. *Phys. Rev. Lett.* 82, 3372{3375.
77. Jang, H., Hall, C. K. & Zhou, Y. Q. (2002). Protein folding pathways and kinetics: molecular dynamics simulations of beta-strand motifs. *Biophys. J.* 83, 819{835.
78. Cieplak, M. & Hoang, T. X. (2001). Kinetic nonoptimality and vibrational stability of proteins. *Proteins: Struct. Func. & Genet.* 44, 200{25.
79. Shimada, J., Kussell, E. L. & Shakhnovich, E. I. (2001). The folding thermodynamics and kinetics of crambin using an all-atom Monte Carlo simulation. *J. Mol. Biol.* 308, 79{95.
80. Hoang, T. X. & Cieplak, M. (2000). Sequencing of folding events in G α -type proteins. *J. Chem. Phys.* 113, 8319{8328.
81. Zhou, Y. Q. & Karplus, M. (1999). Folding of a model three-helix bundle protein: a thermodynamic and kinetic analysis. *J. Mol. Biol.* 293, 917{951.
82. Alder, B. J. & Wainwright, T. E. (1959). Studies in molecular dynamics. I. general method. *J. Chem. Phys.* 31, 459{466.
83. Zhou, Y. Q., Karplus, M., Wichert, J. M. & Hall, C. K. (1997). Equilibrium thermodynamics of homopolymers and clusters: molecular dynamics and Monte Carlo simulations of systems with square-well interactions. *J. Chem. Phys.* 106, 10691{10708.
84. Allen, M. P. & Tildesley, D. J. (1987). Computer simulation of liquids. Clarendon Press, Oxford.
85. Rapaport, D. C. (1997). The art of molecular dynamics simulation. Cambridge University Press, Cambridge.
86. Grosberg, A. Y. & Khokhlov, A. R. (1997). Giant molecules. Academic Press, Boston.
87. Dokholyan, N. V., Buldyrev, S. V., Stanley, H. E. & Shakhnovich, E. I. (1998). Molecular dynamics studies of folding of a protein-like model. *Folding & Design*, 3, 577{587.
88. Dokholyan, N. V., Buldyrev, S. V., Stanley, H. E. & Shakhnovich, E. I. (2000). Identifying the protein folding nucleus using molecular dynamics. *J. Mol. Biol.* 296, 1183{1188.

Figure 1: (a) Upper triangle: contact map with 160 native contacts. The secondary structure elements are the clusters of contacts that are organized perpendicularly to the map diagonal. Long-range contacts between the two termini are enclosed in the circle, and long-range contacts between the RT-loop and the distal hairpin are enclosed in the square. Lower triangle: the frequency map for the initial set of 1100 unfolded conformations at $T = 1.0$. (b) Frequency map of the unfolded state at $T = T_F = 0.626$. We compute the frequencies for a particular folding transition, whose potential energy trajectory we show in the inset (see Methods). Same for (c) $T = 0.54$ and (d) $T = 0.33$, the lowest temperature studied.

Figure 2: (a-e) Histograms of folding times for selected temperatures. At $T = 0.33$ and $T = 0.36$, the two lowest temperatures studied, histograms have a maximum for long folding times ($\#^A$), which suggests the existence of putative intermediates. At $T = 0.33$, a maximum in the histogram ($\#^T$), not present at $T = 0.36$, corresponds to short lived kinetic traps. The distributions of folding times are unimodal at higher temperatures. At $T = 0.54$, the histogram is compact, and has no tail of long folding times. At $T = 0.64$, the histogram fits a single-exponential distribution $e^{-t/\tau_F} = e^{-t/\tau_F} = e^{-t/\tau_F}$ for times larger than the relaxation time of 1500 t.u. (dashed line). We estimate the errors of the histogram bars as the square root of each bar. (f) Average folding time versus temperature. Each dot represents the folding time for a particular folding transition. (g) Ratio of the average and the standard deviation, $r = \tau_F / \sigma_F$, for the distribution of folding times. The ratio approaches one above T_{KP} and zero below T_{KP} . The ratio is maximal at T_{KP} , indicating a compact distribution of folding times at this temperature.

Figure 3: (a) Distributions of the potential energies of the slow folding pathways for temperatures below $T = 0.43$. The distributions are bimodal, suggesting two putative intermediates I_1 and I_2 . (b) The potential energy of the distribution peaks ($*$ and $\#$) increases with temperature, but the energy difference between peaks remains constant. The energy of the peaks is significantly larger than the equilibrium energy of the folded state (4). (c) Distributions of survival times at $T = 0.33$ for the high energy intermediate I_1 ($*$), $\tau_{F,i} = 1.81 \cdot 10^6$ and $\tau_{F,i} = 1.85 \cdot 10^6$, and the low energy intermediate I_2 ($\#$), $\tau_{F,i} = 2.47 \cdot 10^6$ and $\tau_{F,i} = 2.43 \cdot 10^6$, fit to single-exponential distributions. (d) Arrhenius plot of the average survival time of intermediate I_2 below

$T = 0.44$. This upper bound temperature coincides with the temperature below which the distribution of the potential energies (Fig. 3a) of the slow folding pathways becomes bimodal. (e) Upper triangle: Absent contacts (filled squares) and present contacts (crosses, $\setminus C_4$) in intermediate I_1 . Upon the transition $I_1 \rightarrow I_2$, these contacts reverse their presence (so that the filled squares are the present contacts and the crosses are the absent contacts). There are more squares than crosses, which roughly accounts for the difference of six energy units between the two intermediates. Lower triangle: long-range contacts $\setminus C_1$ are present in intermediate I_1 , and long-range contacts $\setminus C_2$ are absent. There are 23 contacts in $\setminus C_1$ and 15 contacts in $\setminus C_2$. (f) Probability that a folding transition at $T = T_{KP} = 0.54$ contains a protein conformation with similarity S to intermediate I_1 (see Methods).

Figure 4: Schematic diagram of fast and slow folding pathways. At $T = 0.33$, approximately in 15% of the simulations, the model protein undergoes a folding transition through the slow folding pathways. We show the protein structure in I_1 and I_2 using the secondary structural elements of the native state, although some of these elements are not formed. In intermediate I_1 , both termini and the strand A form a β -sheet (in the ellipse). The corresponding set of native contacts is C_1 . Dissociation of the β -sheet leads to rearrangements of the protein conformation and successful folding to the native state (NS). However, dissociation of the distal hairpin (in red) leads to more localized rearrangements that may lead the protein to intermediate I_2 . Upon $I_1 \rightarrow I_2$ transition, contacts of C_2 (the two ellipses in I_2) form, but contacts of C_4 (the ellipse in NS) break.

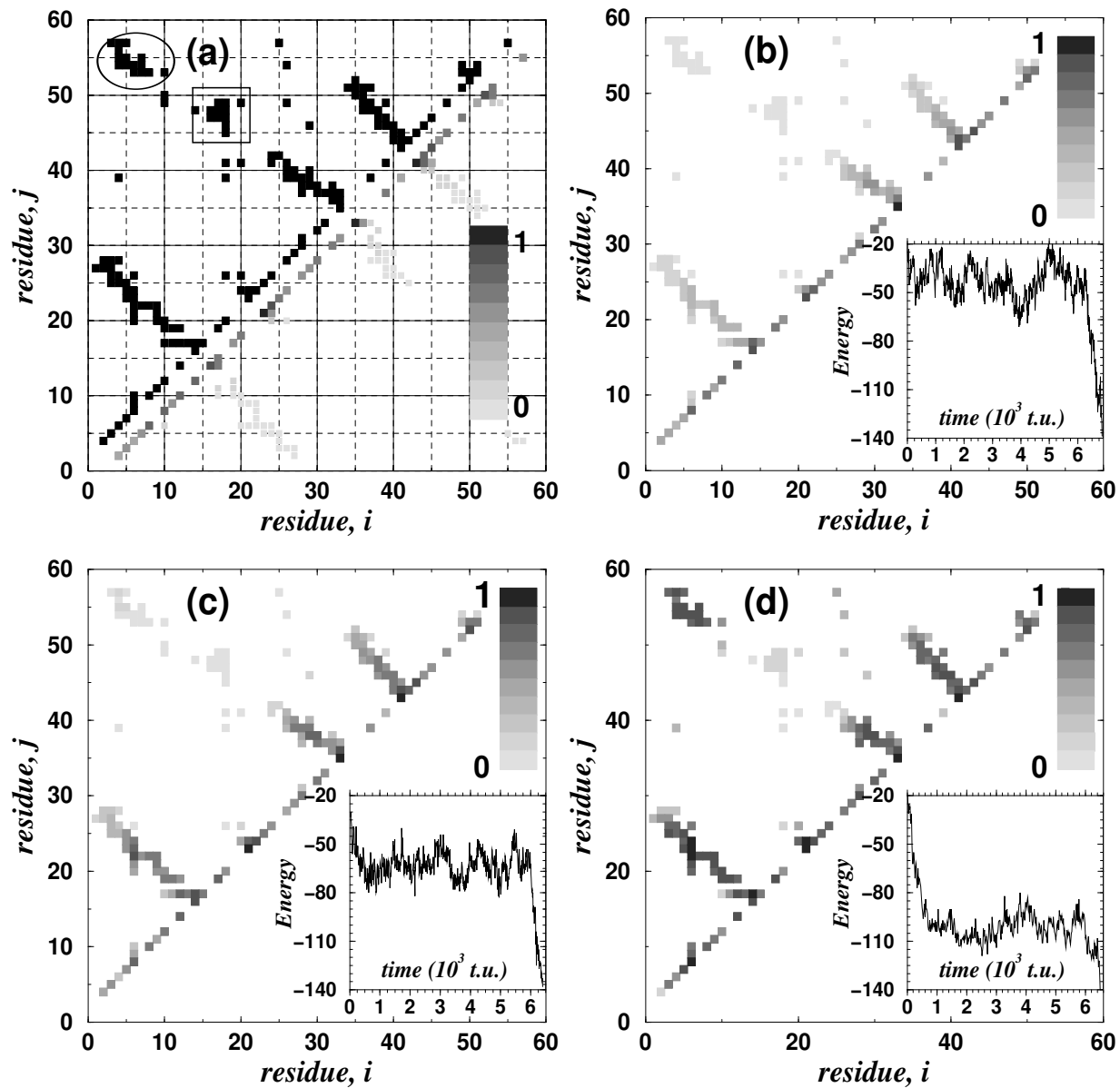


Figure 1:

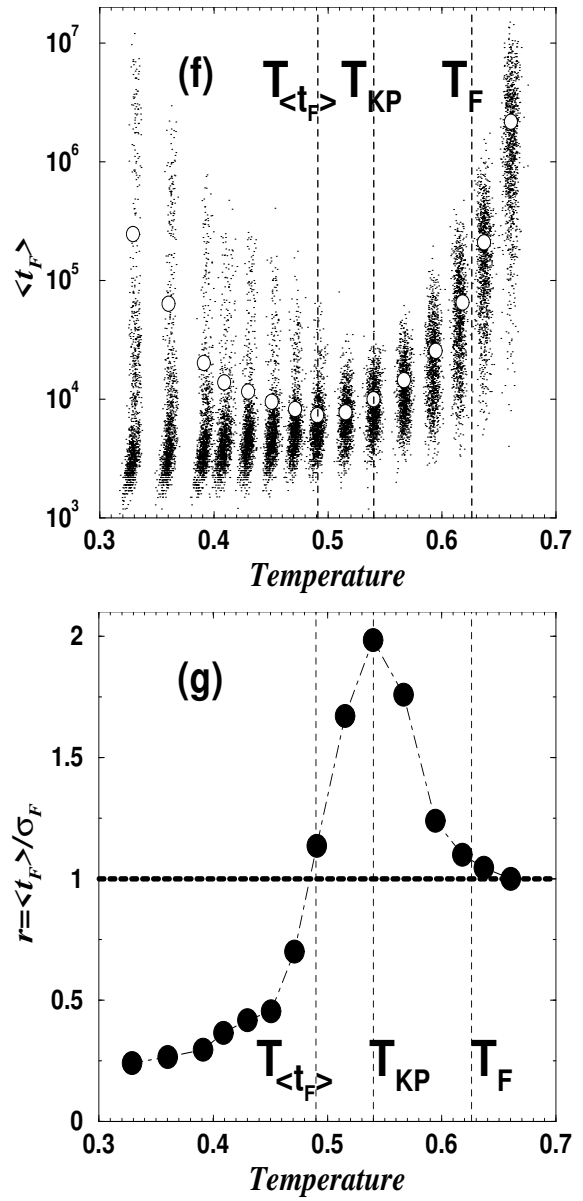
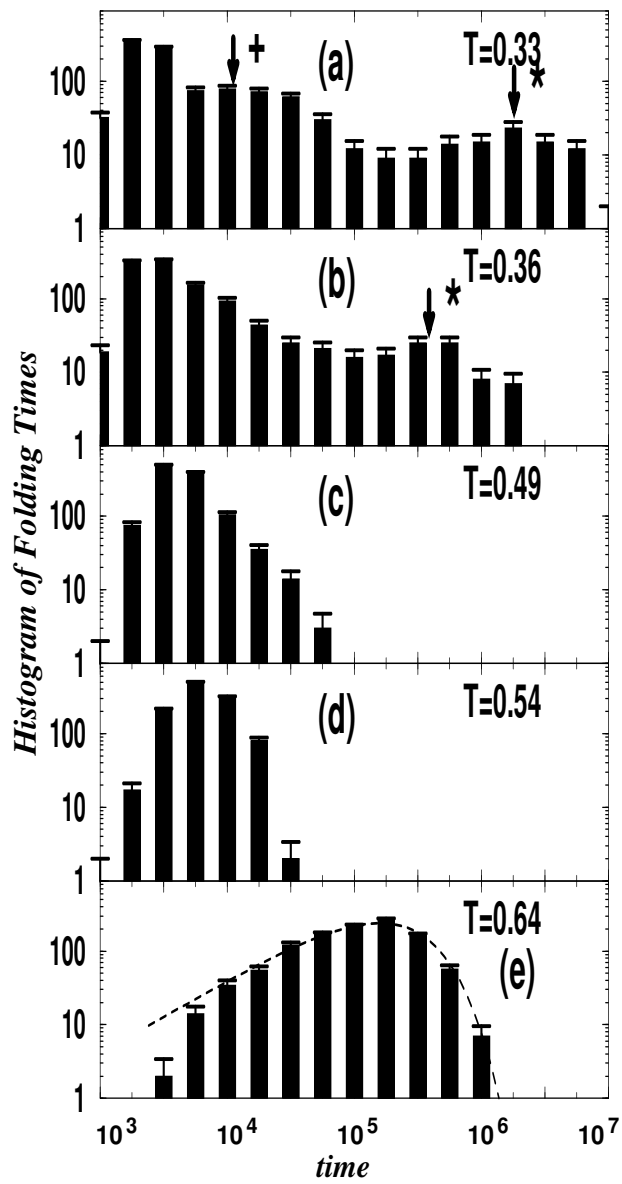
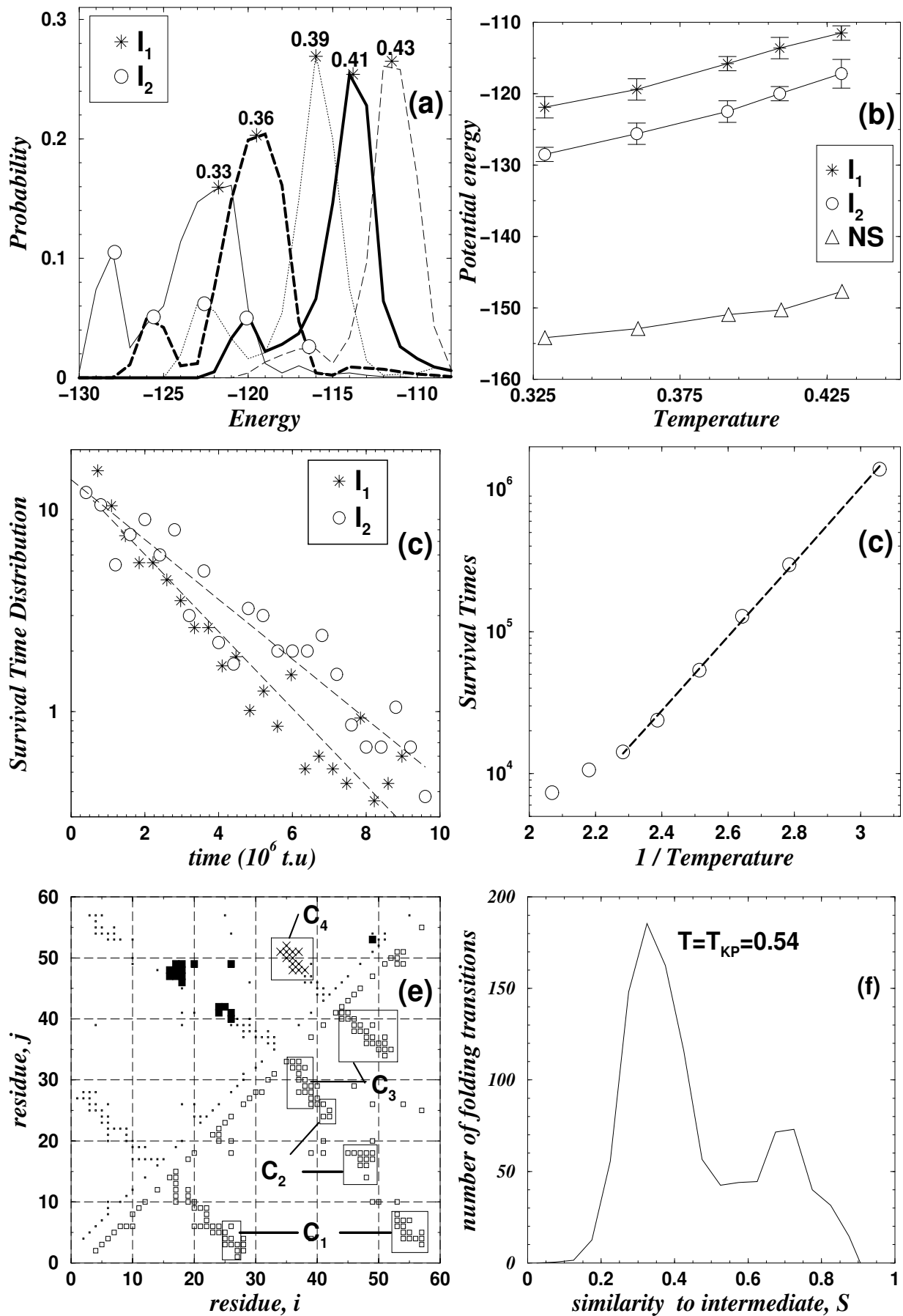


Figure 2:



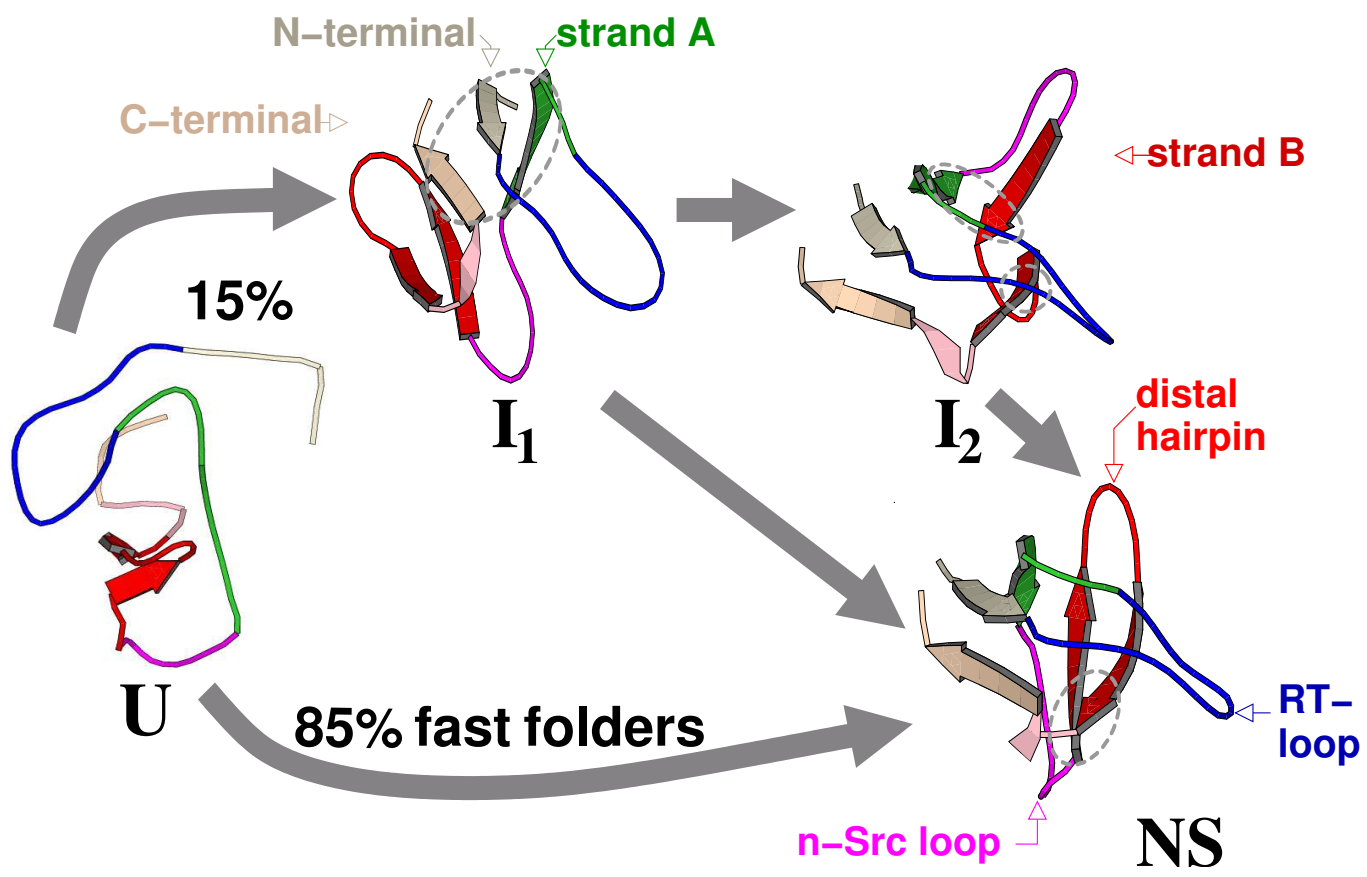


Figure 4: